Iraqi Journal of Physics, 2025
https://doi.org/10.30723/ijp.v23i1.1308

Vol.23, No.1, PP.56-67
P-ISSN: 2070-4003
E-ISSN: 2664-5548

Characterization of Arc Mg and Mg/C Plasmas Generated by Electrical Explosion Strips

Anfal M. Gubair[1a*] and Saba. J. Kadhem[1b]
[1]*Department of Physics, College of Science, University of Baghdad, Baghdad, Iraq*
[a*]Corresponding author: anfal.m@sc.uobaghdad.edu.iq

Abstract
This research investigates the properties and behaviour of magnesium (Mg) and magnesium/carbon (Mg/C) plasmas generated using the electric explosion strips technique, a method noted for producing large quantities of nanomaterials and generating plasma in confined environments. Plasma was created by passing high current densities through a metal stripe immersed in distilled, deionized water, leading to rapid ionization. Optical Emission Spectroscopy (OES) was employed to analyse the plasma properties, as it preserves the original state of the plasma and allows for detailed characterization based on emitted optical spectra. Key parameters, including electron temperature (T_e) and electron density (n_e), were determined using the Boltzmann diagram and Stark broadening method, respectively. The study observed that increasing exploding current, ranging from 25 to 125 A, enhanced the ionization processes, leading to higher electron temperatures and densities. T_e increases from 0.71 to 0.97 eV and n_e increases from 21.41×10^{16} to 25.37×10^{16} cm^{-3} for magnesium plasma. At the same current value, T_e climbed from 0.92 to 1.10 eV, and the electron density increased from 11.5×10^{17} to 19.7×10^{17} cm^{-3} when the magnesium bar detonated together with the carbon rod. The findings highlight the significant effect of detonation current on plasma properties, which is attributed to enhanced heating mechanisms and increased ionization, contributing to higher electron densities and temperatures.

Article Info.

Keywords:
Arc Discharge Plasma, Plasma Parameters, Optical Emission Spectroscopy, Electron Density, Electron Temperature.

Article history:
Received: May, 30, 2024
Revised: Oct. 03, 2024
Accepted: Oct. 21, 2024
Published:Mar. 01,2025

1. Introduction
The electrical explosive wire (EEW) method has become quite popular recently since it can synthesize different nanomaterials in large quantities [1] and can generate and confine plasma [2]. Plasma is generated by passing a high current density through a metal stripe in contact with a metal stripe. The entire assembly is immersed inside a liquid, where the explosion occurs. Immediately after the explosion, the part of the tape in contact with the metal stripe turns into a plasma state, and a mixture of liquid and vapor quickly forms the explosive material [1]. Optical emission spectroscopy is considered one of the most important experimental methods used to determine and diagnose the properties of the generated plasma [3]. There are many techniques for plasma generation, for example laser deposition, DC sputtering, and Rf sputtering [4-6]. To investigate and comprehend the effects of various physical processes and ascertain their influence, one must be aware of the properties of the plasma being studied [7]. Spectroscopy is a technique that, when applied, leaves the plasma in its original state and structure because it uses the identification of the optical beam that the plasma under study emits and the description of its properties using that beam [8, 9]. To do a spectrum analysis, you need a spectrograph and a detector to resolve and find plasma light. The resulting plasma spectrum can be used to determine element composition and other quantitative and qualitative information [10]. The electron density (n_e) and plasma

temperature (T_e) can be determined using the lengths, shapes, and variations of the emission lines in the plasma spectrum [11]. Two additional features of plasma, the relative energy level populations and the particle speed distribution, can also be explained and predicted using the primary thermodynamic parameter, plasma temperature [12, 13].

The Boltzmann diagram can be used to calculate T_e [14-16]:

$$T_e = \frac{(E_2 - E_1)}{k\ln\frac{(I_1\lambda_1 A_2 g_2)}{(I_2\lambda_2 A_1 g_1)}} \quad (\mathbf{1})$$

where: A_1g_1 and A_2g_2 are the transition strengths for the first and second wavelengths, respectively, and k is Boltzmann's constant. The intensity of the first wavelength peak in the plasma spectrum is represented by I_1, the intensity of the second wavelength peak by I_2, and the energies of the first and second wavelength peaks in the plasma spectrum are represented by E_1 and E_2, respectively [17]. The following formula is used to obtain the electron density n_e in (cm^{-3}) as a result of Stark broadening [18]:

$$n_e = \frac{I_1}{I_2^*} 6.04 \times 10^{21} (T_e)^{3/2} e^{\frac{(E_1 - E_2 - X_z)}{kT}} \quad (\mathbf{2})$$

where

$$I_2^* = \frac{I_2\lambda_2}{g_2 A_2} \quad (\mathbf{3})$$

During the ionization stage, the species ionization energy is denoted as E with a unit of eV, X_z means energy difference between level 2 and level 1, and Z stands for the species ionization phase. The shielding confers quasi-neutrality, a unique characteristic of plasma. To compute a distance (λ_D), also called the Debye length, the following formula is used [19, 20]:

$$\lambda_D = \left(\frac{\varepsilon_o k T_e}{n_e e^2}\right)^{1/2} = 742 \times \left(\frac{T_e}{n_e}\right)^{1/2} \quad (\mathbf{4})$$

where: e is the electron charge, and ε_o is the permittivity of free space. The following equation yields the number of particles (N_D) inside the Debye sphere [21-23]:

$$N_D = \frac{4\pi}{3} n_e \lambda_D^3 \quad (\mathbf{5})$$

While plasma frequency (f_p) is calculated from the equation [24]:

$$f_p \approx 8.98\sqrt{n_e}(\text{Hz}) \quad (\mathbf{6})$$

Frequency is one of the fundamental properties of plasma [25]. This frequency, which depends only on the plasma density, is one of the fundamental parameters of plasma. Because of the smallness of m, the plasma frequency is usually very high [26].

This work aims to diagnose two types of plasma (Mg and Mg/C plasma) generated using the explosive tape technique at five values of the detonation current, calculate their parameters by analyzing the optical spectra of both types and compare the two types of plasma parameters with each other.

The novelty of this study lies in using the EEW method to generate Mg and C nanoparticles. This method allows for the generation of large quantities of nanomaterials. It confines the plasma within a liquid medium, resulting in distinct plasma properties that have not been extensively studied before. Also, the novelty of this work lies in the detailed characterization of Mg and Mg/C plasmas using optical emission spectroscopy (OES) at varying detonation currents, providing new insights into the relationship between current density and plasma parameters. In addition, this study contributes to the understanding of the mechanisms of ionization and enhanced heating in confined plasma environments, a topic that remains relatively unexplored in the current literature.

2. Experimental Work

The system used in this work consisted of a power supply (type Edon MMA-250S, manufactured in China) generating direct current with a voltage of 82 V. The system was powered by a high current within the range of (0 - 250) A, and a beaker containing 100 ml of Double-Distilled Deionized Water (DDDW). The pH of the water was 6.5, and its conductivity was about 0.5 microsiemens. A magnesium plate (99.99% purity) with 2 cm width and 3 cm length was immersed inside the distilled water in the beaker to generate magnesium plasma. A magnesium plate connected to the power supply's positive end was the first electrode, and the second electrode was a magnesium stripe, connected to the power supply's negative end. Magnesium plasma is generated when the magnesium stripe comes into contact with the plate, pushing huge amounts of energy through the stripe. The energy entering the system exceeds the evaporation energy of the stripe material. The time taken for the current to propagate through the stripe is less than the time for power input. Consequently, the tape melts and evaporates, and ionization and agitation processes for the atoms of the medium occur, resulting in magnesium plasma.

The system used to generate carbon/magnesium plasma consisted of a vertical carbon rod (99.98% purity) 6 cm long and 1 cm in diameter representing the positive electrode. It was installed vertically in a beaker containing DDDW. The negative electrode was the magnesium strip. When contact occurs between the two electrodes, very high energy flows, causing the substance to melt, evaporate, and transform into a plasma state. The carbon and magnesium plasma spectrum were recorded at five blast current values 25, 50, 75, 100, and 125 A. Optical emission spectroscopy is an effective method for plasma diagnosis. The spectra were captured utilizing an S3000-UVNIR spectrometer manufactured in China. This spectrometer has essential components including SubMiniature Version A fiber (SMA fiber), charge-coupled device (CCD), and an optical system. It measured the properties of Mg and C/Mg plasma produced using explosive wires in distilled water. The data was examined and matched with the National Institute of Standards and Technology NIST data [27]. The wire explosion system's schematic diagram is displayed in Fig. 1.

3. Results and Discussion

Fig. 2 displays the optical emission spectra (OES) of carbon-containing magnesium plasma at five different currents. Numerous peaks for different elemental atoms and ions can be seen in the spectrum; however, the two most significant peaks for magnesium atoms and ions are located at 435.19 and 546.00 nm. A few peaks emerged, corresponding to hydrogen, oxygen, magnesium, and carbon. The breakdown of two water molecules is the source of the hydrogen atom peak. The spectra were recorded in the range 350-1000 nm. It is evident from the spectra that when the current density rises, the peak intensities do as well [28].

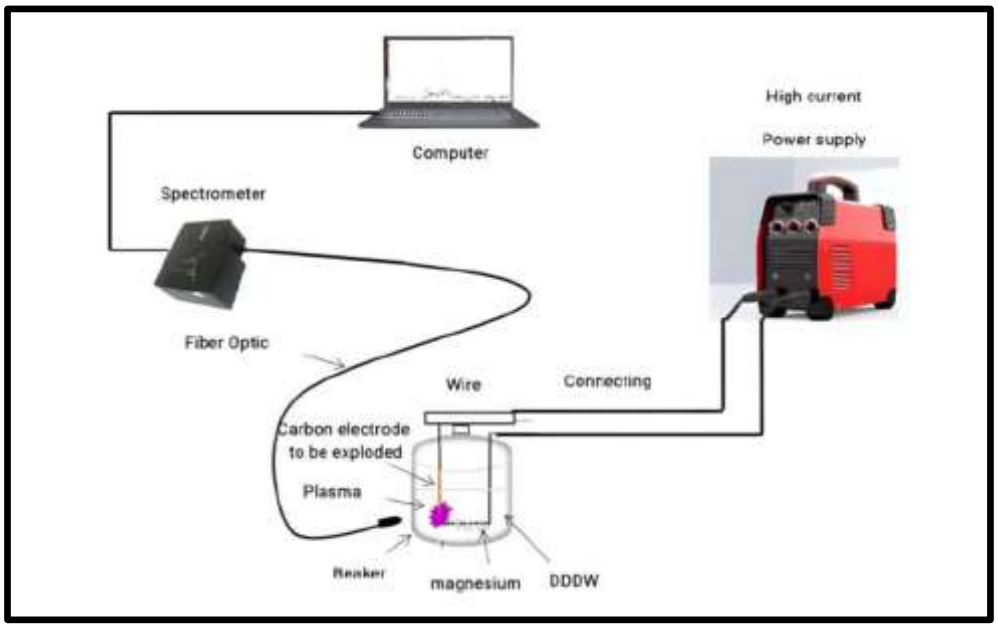

Figure 1: Schematic Diagram of the wire-exploding device.

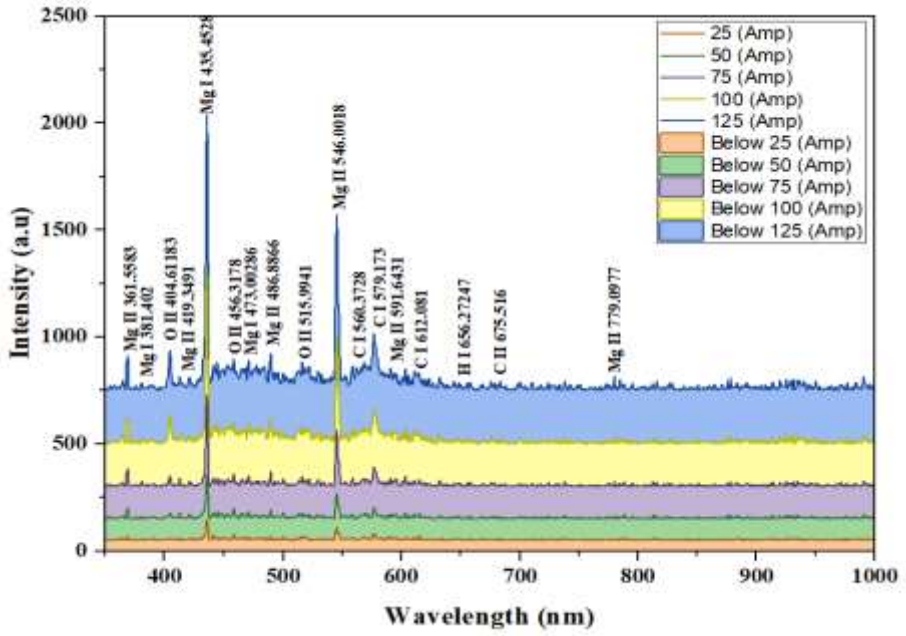

Figure 2: Mg/C plasma emission spectrum for different values of electrical currents 25, 50, 75, 100 and 125 A.

Fig. 2 displays the OES of the plasma produced between 350 and 1000 nm when magnesium nanowires are shot at various DC currents of 25, 50, 75, 100, and 125 A. Strong atomic and ionic emission lines can be seen in the spectra (MgII, MgI, HI, OII and OI) [9]. A small peak corresponding to the magnesium atoms is seen at 453.19 nm and the MgII, ion at 564.00 nm. Due to the dissociation of water molecules, tiny peaks arise at approximately 656.27 nm, corresponding to the hydrogen atoms' Hα line, and at 645.36 nm, corresponding to oxygen atoms. The spectra show that an increase in current density causes the peaks' intensity to rise. This result is consistent with previous studies [2, 8].

It is evident from all of the spectra displayed in Figs. 2 and 3 that raising the current density have caused the peak intensities to rise. The increase in current density increases the energy provided to the atoms, which in turn causes an increase in the ionization process or an increase in n_e. Figs. 4 and 5 of the magnesium atoms spectrums have peak line profiles of 435.190 nm for Mg/C and Mg plasma, respectively. The full width at half maximum (FWHM) was used to calculate the electron density for the Mg/C plasma and the variable current Mg plasma using the Lorentzian fitting and the Stark effect, based on the usual expansion values for this line. It is evident that FWHM narrowed as the current dropped, indicating a drop in electron density [14, 17].

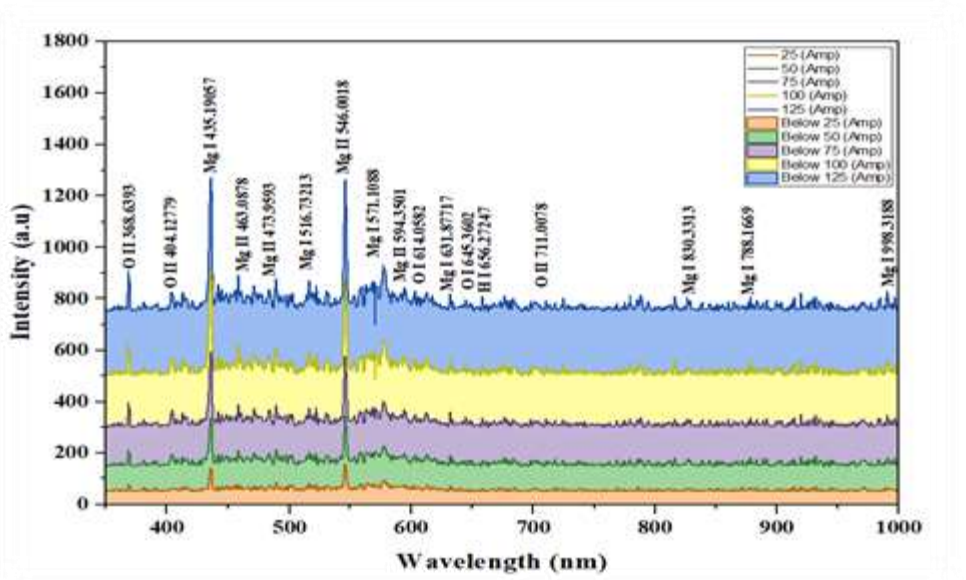

Figure 3: Mg plasma emission spectra for different values of electrical currents 25, 50, 75, 100, and 125 A.

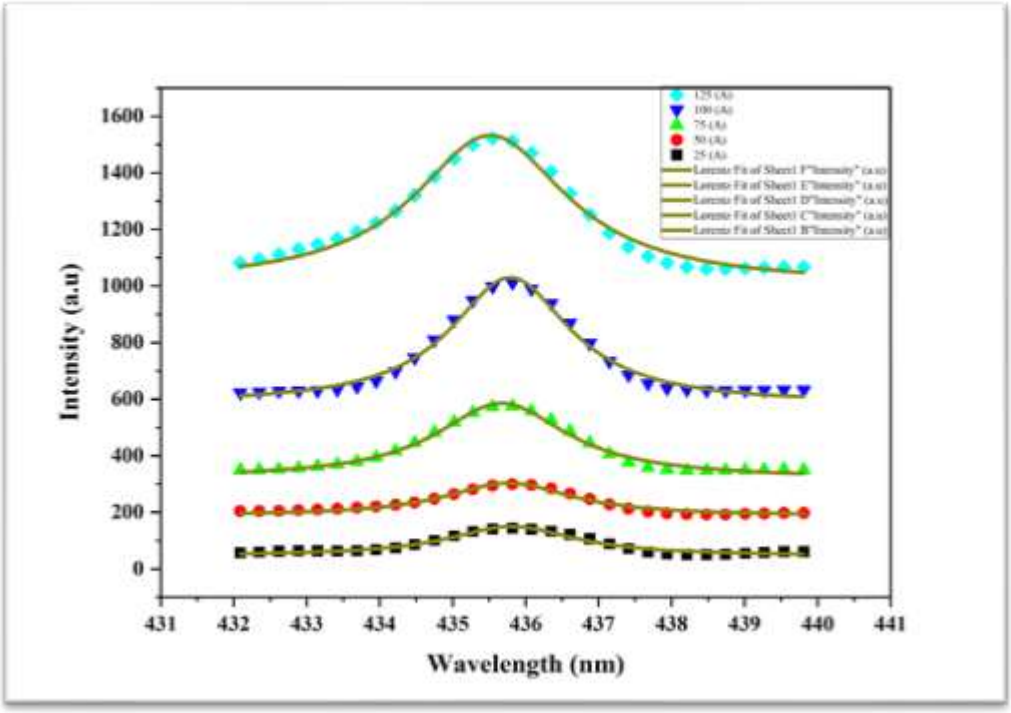

Figure 4: Broadening of the 435.4628 nm M_g peak and its Lorentzian structure for M_g/C with different currents 25, 50, 75, 100, and 125 A.

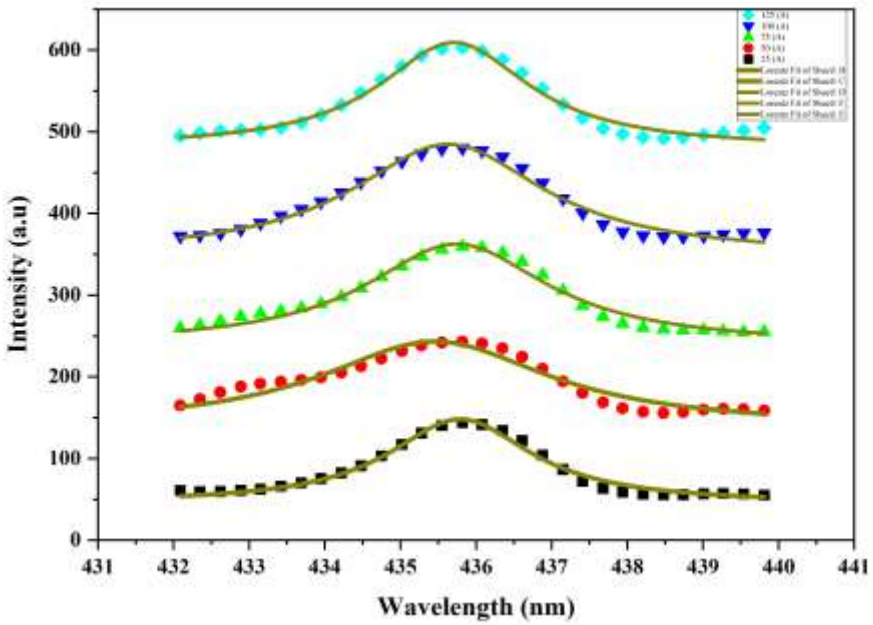

Figure 5: Broadening of the 435.9057 nm M_g peak and its Lorentzian structure for M_g/C with different currents 25, 50, 75, 100, and 125 A.

The plasma was assumed to be in a state of local thermodynamic equilibrium (LTE) with many excited atoms to compute the plasma's parameters. The Boltzmann plot's best linear slope was used to calculate the electron temperatures. The atomic species and ionization stage from which the peaks in a Boltzmann plot originate must be the same. The energy of upper levels, statistical weights, and transition probabilities of each element were taken from the NIST database and used in the experimental plots. The reciprocal of the fitting line's slope is the electron temperature, as Fig. 6 illustrates. R^2, a statistical measure of linear fit, ranges from 0 to 1, with a value around 1 representing the best fit. The values of different parameters for Mg/C plasma are shown in Tables 1 and 2). These parameters include T_e, FWHM, n_e, f_e, λ_D, and N_D for different current values 25, 50, 75, 100, 125 A. Figs. 6 and 7, it is noted that T_e in Mg/C plasma increased from 0.92 to 1.10 eV, and the electron density increased from 11.5×10^{17} to 19.7×10^{17} cm^{-3} with increasing current; For Mg plasma, T_e increased from 0.71 to 0.97 eV and n_e increases from 21.41×10^{16} to 25.37×10^{16} cm^{-3}. As the current value increased, both the electron temperature and density increased. The graphs and tables show that the increase in electron temperature and density brought on by the increase in electrical current results from plasma particles absorbing energy. This result is consistent with previous studies [14, 20].

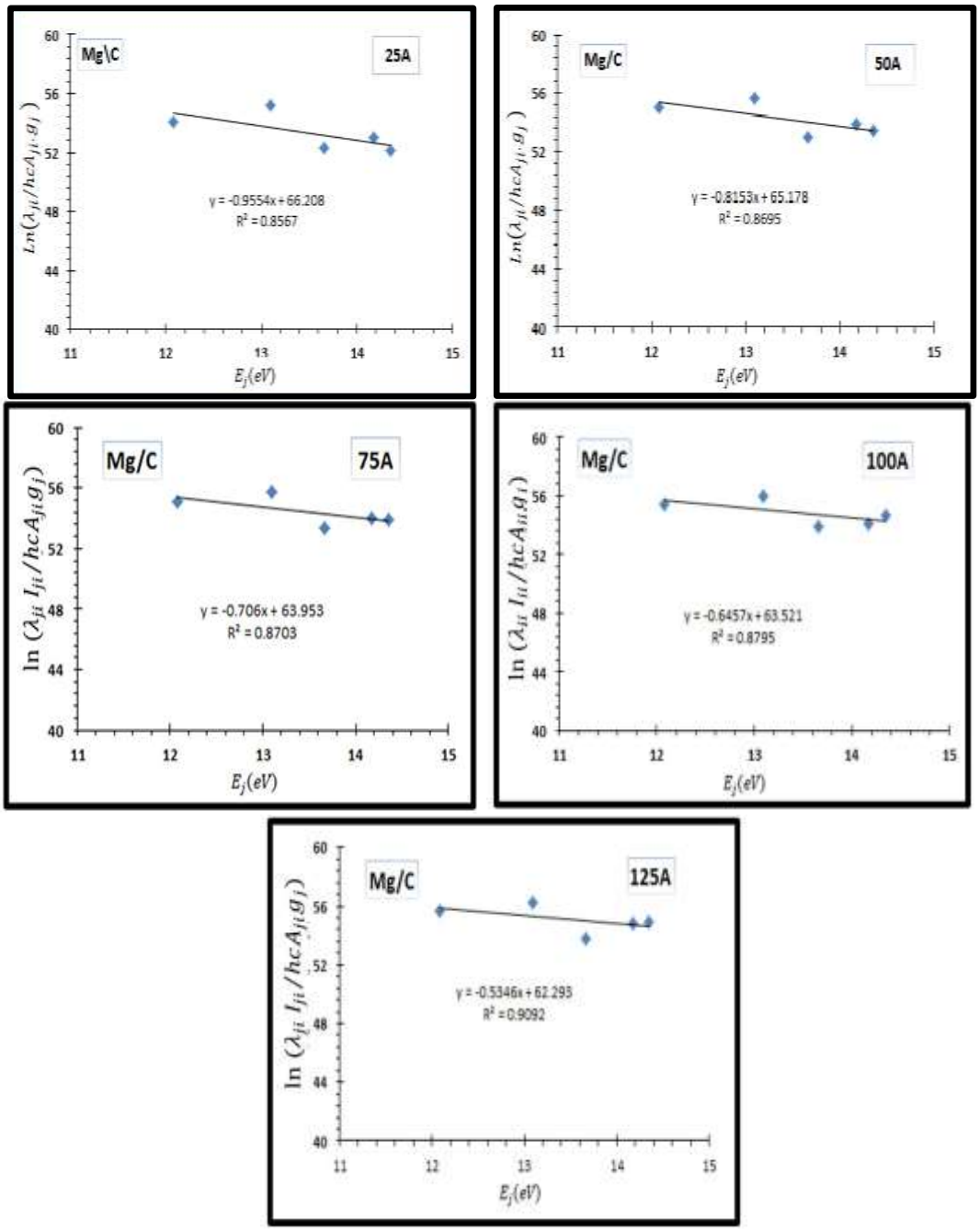

Figure 6: Boltzmann- plot of magnesium emmited lines, generated at different currents by EEW.

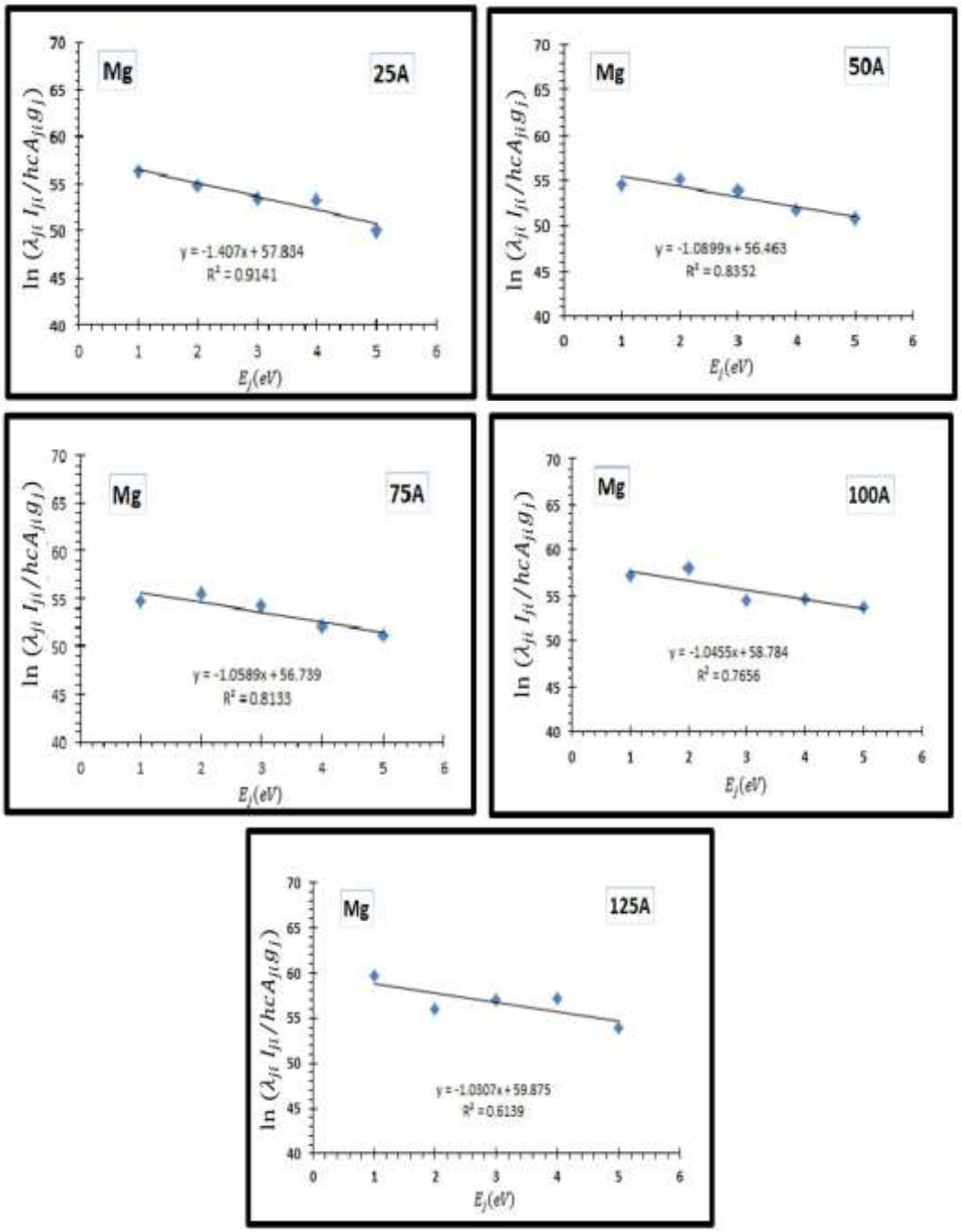

Figure 7: Boltzmann-plot of magnesium lines, generated at different currents by EEW.

Figs. 8 and 9 represent the change in electron temperature T_e and the electron density n_e For Mg/C plasma and Mg plasma, respectively. The change in plasma parameters as the detonation current changes is shown in Tables 1 and 2. When the detonation current increases in this process, several factors contribute to the rise in T_e and n_e. The increased energy from the high current can enhance the heating mechanisms within the plasma. These mechanisms include Joule heating (heating due to electrical resistance), collision heating (heating due to collisions between charged particles), and radiative heating (heating due to the emission and absorption of photons). Also, a higher detonation current means delivering more energy to the conductive tape, which leads to a more intense explosion and, thus, more vaporized materials. Increasing the energy input leads to higher temperatures inside the plasma. An increase in current causes an increase in the free electrons density. High currents increase the ionization of the evaporated substance and, thus, increase the process of liberating electrons from atoms. This means that the center of the plasma becomes rich in free electrons. The shock wave resulting from the explosion also causes pressure inside the plasma and, thus, a rapid expansion of the vaporized substance, which increases the numerical density of ions and electrons. The Mg/C plasma has a higher electron temperature and electron density value than the Mg plasma. With the increase of the current, T_e for Mg/C plasma increases from 0.92 to 1.10 eV, while for Mg plasma, Te increases from 0.71 to 0.97 eV. Also, as the current increases, ne for Mg/C plasma increases from 11.5×10^{17} to 19.7×10^{17} cm^{-3} and n_e for Mg/C plasma increases from 21.41×10^{16} to 25.37×10^{16} cm^{-3} in the case of magnesium plasma. These higher values in Mg/C plasma are due to the presence of carbon, which enhances ionization and heating mechanisms, resulting in more energy absorption, higher electron temperature, and greater electron density.

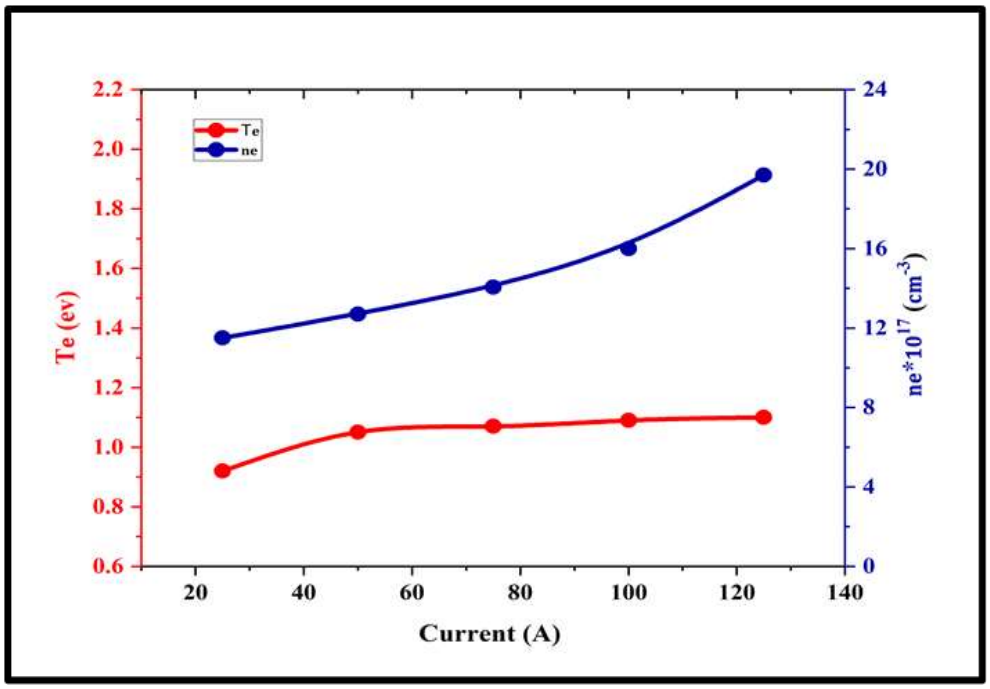

Figure 8: Variation of T_e and n_e with current for Mg/C plasma.

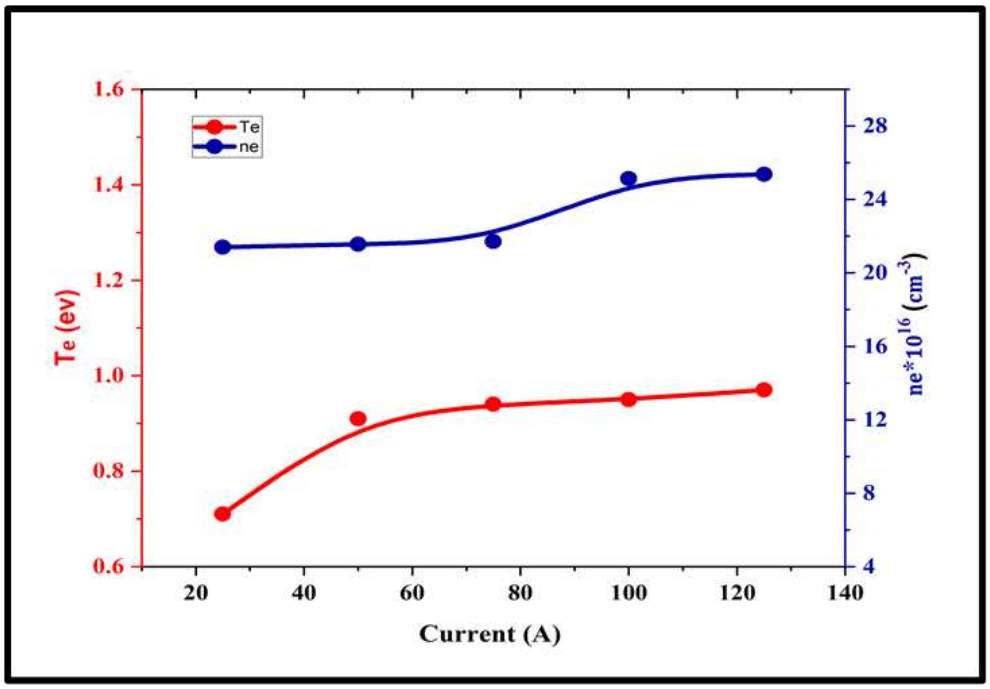

Figure 9: Variation of T_e and n_e with current for Mg plasma with current.

Table 1: Parameters of Mg/C plasma for the various current values.

Current (A)	T_e (eV)	$n_e \times 10^{17}$ (cm^{-3})	$f_p \times 10^{13}$ (Hz)	$\lambda_D \times 10^{-6}$ (cm)	N_D
25	0.92	11.5	21.41	1.890	4074
50	1.05	12.7	21.48	2.010	4936
75	1.07	14.05	21.55	2.015	5007
100	1.09	16	23.20	1.896	4832
125	1.10	19.7	23.30	1.891	4832

Table 2: Mg plasma parameters at various current values.

Current (A)	T_e (eV)	$n_e \times 10^{16}$ (cm^{-3})	$f_p \times 10^{13}$ (Hz)	$\lambda_D \times 10^{-6}$ (cm)	N_D
25	0.71	21.41	26.15	1.353	2232
50	0.91	21.56	26.24	1.532	3263
75	0.94	21.71	26.33	1.549	3395
100	0.95	25.14	28.34	1.448	3216
125	0.97	25.37	28.47	1.452	3271

4. Conclusions

In this work, the properties of Mg and Mg/C plasmas generated by the electrically explosive tape method were diagnosed and studied. The results of optical emission spectroscopy demonstrated that T_e and n_e increased with increasing detonation current. The increase in temperature and electron density is due to the enhanced heating mechanisms within the plasma medium, including radiation heating, collision heating, and joule heating. High detonation currents also led to increased ionization of the vaporized material, increasing the density of free electrons inside the plasma. The rapid expansion of the explosive material also contributed to the effects of pressure inside the plasma, increasing the density of electrons and ions.

Conflict of Interest

The authors declare that they have no conflict of interest.

References

1. S. Singh and N. Goswami, Int. J. Mat. Res. **114**, 738 (2023). DOI: doi:10.1515/ijmr-2021-8713.
2. S. M. Fathi and S. J. Kadhim, Iraqi J. Sci. **63**, 163 (2022). DOI: 10.24996/ijs.2022.63.1.17.
3. H. B. Baniya, R. Shrestha, R. P. Guragain, M. B. Kshetri, B. P. Pandey, and D. P. Subedi, Int. J. Poly. Sci. **2020**, 9247642 (2020). DOI: 10.1155/2020/9247642.
4. K. A. Aadim Ph D and A. S. Jasim Ph D, Karbala Int. J. Mod. Sci. **8**, 71 (2022). DOI: 10.33640/2405-609X.3210.
5. H. J. Imran, K. A. Hubeatir, K. A. Aadim, and D. S. Abd, J. Phys.: Conf. Ser. **1818**, 012127 (2021). DOI: 10.1088/1742-6596/1818/1/012127.
6. R. S. Mohammed, K. A. Aadim, and K. A. Ahmed, Karbala Int. J. Mod. Sci. **8**, 88 (2022). DOI: 10.33640/2405-609X.3225.
7. X. Lu, Z. Xiong, F. Zhao, Y. Xian, Q. Xiong, W. Gong, C. Zou, Z. Jiang, and Y. Pan, Appl. Phys. Lett. **95**, 181501 (2009). DOI: 10.1063/1.3258071.
8. M. J. Ketan and K. A. Aadim, Iraqi J. Sci. **64**, 188 (2023). DOI: 10.24996/ijs.2023.64.1.19.
9. M. H. Suhail, K. A. Adim, and A. H. Wanas, Curr. J. Appl. Sci. Tech. **7**, 263 (2015). DOI: 10.9734/BJAST/2015/14876.
10. M. H. Kabir, M. L. Guindo, R. Chen, A. Sanaeifar, and F. Liu, Foods **11**, 2051 (2022). DOI: 10.3390/foods11142051.
11. M. Al-Salihi, R. Yi, S. Wang, Q. Wu, F. Lin, J. Qu, and L. Liu, Opt. Expr. **29**, 4159 (2021). DOI: 10.1364/OE.410878.
12. K. A. Aadim, A. Z. Mohammad, and M. A. Abduljabbar, IOP Conf. Ser.: Mater. Sci. Eng. **454**, 012028 (2018). DOI: 10.1088/1757-899X/454/1/012028.
13. D. A. Cremers and L. J. Radziemski, *Handbook of Laser-Induced Breakdown Spectroscopy* (West Sussex, UK, John Wiley & Sons, 2013).
14. Z. M. Hasan and Q. A. Abbas, Iraqi J. Appl. Phys. **20**, 19 (2024).
15. A. F. Ahmed, Iraqi J. Phys. **17**, 103 (2019). DOI: 10.30723/ijp.v17i42.438.
16. K. A. Aadim, Iraqi J. Phys. **14**, 122 (2019). DOI: 10.30723/ijp.v14i31.179.
17. T. Mieno, *Plasma Science and Technology: Progress in Physical States and Chemical Reactions* (Rejeka, Croatia, InTech, 2016).
18. M. A. Ismail, H. Imam, A. Elhassan, W. T. Youniss, and M. A. Harith, J. Anal. At. Spectrom. **19**, 489 (2004). DOI: 10.1039/B315588A.
19. M. L. Badran and S. J. Kadhem, Iraqi J. Phys. **22**, 10 (2024). DOI: 10.30723/ijp.v22i1.1194.
20. N. K. Hussein and S. J. Kadhem, Iraqi J. Sci. **63**, 2492 (2022). DOI: 10.24996/ijs.2022.63.6.16.

21. Z. M. Hasan and Q. A. Abbas, Iraqi J. Phys. **22**, 31 (2024). DOI: 10.30723/ijp.v22i1.1191.
22. R. S. Mohammed, K. A. Aadim, and K. A. Ahmed, Iraqi J. Sci. **63**, 3711 (2022). DOI: 10.24996/ijs.2022.63.9.5.
23. K. A. Aadim, Iraqi J. Phys. **16**, 1 (2018). DOI: 10.30723/ijp.v16i38.3.
24. Q. A. Abbas, Iraqi J. Sci. **60**, 1251 (2019). DOI: 10.24996/ijs.2019.60.6.8.
25. A. H. Shaker, K. A. Aadim, and M. H. Nida, J. Opt. **53**, 1273 (2024). DOI: 10.1007/s12596-023-01256-0.
26. F. F. Chen, *Introduction to Plasma Physics and Controlled Fusion* (Los Angeles, CA, USA, Springer, 1984).
27. A. Kramida and Y. Ralchenko, Nation. Instit. Stand. Tech. **5.12**, (1999). DOI: 10.18434/T4W30F.
28. A. K. Pathak, N. K. Rai, R. Kumar, P. K. Rai, A. K. Rai, and C. G. Parigger, Atoms **6**, 42 (2018). DOI: 10.3390/atoms6030042.

توصيف بلازمات القوس للمغنيسيوم للمغنيسيوم / كاربون المتولدة بالتفجير الكهربائي للأشرطة

أنفال محمد جبير[1] وصبا جواد كاظم[1]

[1]قسم الفيزياء كلية العلوم جامعة بغداد، العراق

الخلاصة

درس هذا البحث خصائص وسلوك بلازما المغنيسيوم (Mg) والمغنيسيوم/الكربون (Mg/C) المتولدة باستخدام تقنية تفجير الاسلاك، وهي طريقة واعدة لقدرتها على إنتاج كميات كبيرة من المواد النانوية وتوليد البلازما في المناطق المقيدة. تم إنشاء البلازما عن طريق تمرير كثافات تيار عالية عبر شريط معدني مغمور في الماء المقطر منزوع الأيونات، مما يؤدي إلى التأين السريع. تم استخدام التحليل الطيفي للانبعاث البصري (OES) لتحليل خصائص البلازما لأنه يحافظ على الحالة الأصلية للبلازما ويسمح بالتوصيف التفصيلي بناءً على الأطياف الضوئية المنبعثة. تم تحديد المعلمات الرئيسية بما في ذلك درجة حرارة الإلكترون (T_e) وكثافة الإلكترون(n_e)، باستخدام مخطط بولتزمان وطريقة التوسيع ستارك، على التوالي. تبين الدراسة أن زيادة تيار الانفجار (يتراوح من 25 إلى 125 أمبير) عززت عمليات التأين، مما أدى إلى ارتفاع درجات حرارة الإلكترون وكثافته. يزداد (T_e) من (0.71 – 0.97) إلكترون فولت و (n_e) يزيد من (21.41×10^{16} - 25.37×10^{16}) سم$^{-3}$ لبلازما المغنيسيوم. و ارتفعت نفس قيمة التيار (T_e) من (0.92 – 1.10) إلكترون فولت وازدادت كثافة الإلكترونات من (11.5×1017 – 19.7×1017) سم$^{-3}$ عندما انفجر قضيب المغنسيوم مع قضيب الكربون. تسلط النتائج الضوء على التأثير الكبير لتيار التفجير على خصائص البلازما، والذي يعزى إلى تعزيز آليات التسخين وزيادة التأين، والذي بدوره يساهم في ارتفاع كثافات الإلكترون ودرجات الحرارة.

الكلمات المفتاحية: بلازما التفريغ القوسي، معلمات البلازما، التحليل الطيفي للانبعاث البصري، كثافة الإلكترون، درجة حرارة الإلكترون.